

## Design and the operational characteristics of a $16\text{ }\mu\text{m}$ $\text{CF}_4$ laser

P K GUPTA, V P SINGHAL, N S SHIKARKHANE, S SINHA,  
S SASIKUMAR, U NUNDY and U K CHATTERJEE  
Laser Division, Bhabha Atomic Research Centre, Bombay 400 085, India

MS received 23 October 1989

**Abstract.** The design and the operational characteristics of a  $\text{CO}_2$  laser pumped  $\text{CF}_4$  laser developed at BARC are reported. Output energies of up to 20 mJ have been obtained at  $615\text{ cm}^{-1}$  with an absorbed energy conversion efficiency of 10%.

**Keywords.**  $16\text{ }\mu\text{m}$  laser;  $\text{CF}_4$  laser; optically pumped molecular gas laser.

**PACS No.** 42.55

### 1. Introduction

The  $\text{CO}_2$  laser pumped  $\text{CF}_4$  laser is an attractive source for generating step tunable, coherent radiation over  $15.3\text{--}16.3\text{ }\mu\text{m}$  (Gupta and Mehendale 1987). This spectral region overlaps with the  $v_3$  absorption band of  $\text{UF}_6$ , which has a well resolved isotopic shift. The development of  $\text{CF}_4$  laser has therefore received considerable attention for its use in investigations of multi-photon excitation/dissociation of  $\text{UF}_6$  molecules (Tiee and Wittig 1978; Ambartsumyan *et al* 1979; Horsley *et al* 1980; Koren *et al* 1982). We report in this paper the design and operational characteristics of a  $\text{CO}_2$  laser pumped  $\text{CF}_4$  laser, developed at BARC. Output energies of up to 20 mJ have been obtained at  $615\text{ cm}^{-1}$ . The absorbed energy conversion efficiency of 10% obtained in our experiments compares favourably with the best reported for this emission.

### 2. Basic considerations

A schematic energy level diagram for  $\text{CF}_4$  laser (McDowell *et al* 1979) is shown in figure 1. The  $\text{CO}_2$  laser pumps the combination band  $v_2 + v_4$  and lasing occurs on the hot band transition  $v_2 + v_4 \rightarrow v_2$ . The considerable fine structure of the  $\text{CF}_4$  laser bands leads to step tunable emission over 80 lines with a frequency tuning discreteness which can be  $\lesssim 0.1\text{ cm}^{-1}$  (Grasyuk *et al* 1981). It is pertinent to note here that the  $\text{CF}_4$  laser operation is strongly influenced by the characteristics of the pump and the lasing transitions. First, since the pumping is on a dipole forbidden, combination band, the pump absorption is weak. Secondly, the weak pump absorption cannot be offset with an increased operating gas pressure. This is because the lasing band is overlapped with a ground state absorption band ( $v_0 \rightarrow v_4$ ). Due to anharmonicity, the latter is slightly shifted from the lasing band but its broadening creates a significant cavity loss as the pressure increases, limiting laser operation to relatively low pressures

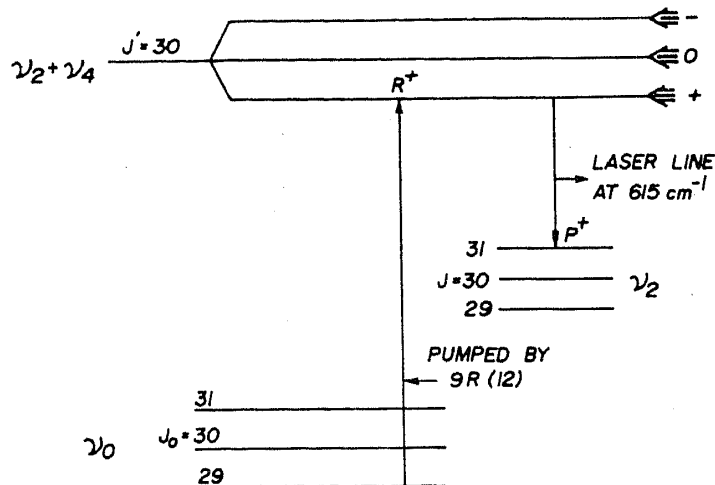


**Figure 1.** Energy level diagram for the  $\text{CF}_4$  laser, with the total angular momentum quantum numbers in the vibrational ground state and in  $v_2 + v_4$  and  $v_2$  denoted by  $J_0$ ,  $J'$  and  $J$  respectively. The three Coriolis sublevels of  $J = 30$  are denoted by  $-$ ,  $0$  and  $+$ . The  $\text{CO}_2$  laser pumps the transition  $R^+$  (29), populating the  $+$  level of  $J' = 30$ ; stimulated emission occurs from this level to  $J = 31$  of  $v_2$ , producing the strong laser line  $P(31)$  at  $615 \text{ cm}^{-1}$ .

(typical operating pressure  $< 10$  torr). Thus long gas columns are necessary to ensure that a significant fraction of the pump energy is deposited in the gas. Gas columns of up to 10 m have been used (Jones *et al* 1978). Further, at the typical operating pressures the absorption spectral width ( $\sim 100$  MHz) is much narrower than the 3–4 GHz bandwidth of the conventional multimode TEA  $\text{CO}_2$  lasers. Efficient optical excitation, therefore, demands spectral narrowing of the  $\text{CO}_2$  pump source, to match the frequency, and the frequency spread, of the absorption feature. Since the  $\text{CF}_4$  absorption feature responsible for  $615 \text{ cm}^{-1}$  emission is nearly resonant (frequency offset  $\sim 19$  MHz) with the line centre of the 9R(12)  $\text{CO}_2$  laser line, the desired pump frequency control is most readily achieved using a hybrid  $\text{CO}_2$  laser (Stein *et al* 1978). Pumping other  $\text{CF}_4$  transitions detuned from the  $\text{CO}_2$  laser line centre requires off-line centre tuning of the  $\text{CO}_2$  laser emission (Stamatakis and Green 1979). It is pertinent to note that spectral control of the TEA  $\text{CO}_2$  laser pump is important not from efficiency considerations alone. The use of multimode pump also leads to an extremely erratic  $\text{CF}_4$  laser operation. For example in the experiments of Green *et al* (1981) with a 3J multimode  $\text{CO}_2$  laser pump and 5 m long  $\text{CF}_4$  gas column, a detectable laser emission was observed in only one out of five pump laser pulses. This arises because for a multimode laser the axial mode frequencies and hence the energy absorbed in the gas changes from pulse to pulse. Finally the laser output has a rather strong temperature dependence primarily because, the lower laser level being close to the ground has significant thermal population. The best performance is obtained at the lowest temperatures compatible with the desired vapour pressure (Green 1979).

Thus, the two major requirements for a  $\text{CF}_4$  laser are a narrow bandwidth  $\text{CO}_2$  laser pump with frequency tuned to the  $\text{CF}_4$  absorption feature and a long cryogenic cell.

### 3. $\text{CO}_2$ Laser pump

A schematic diagram of the home built,  $\text{CO}_2$  laser pump system is shown in figure 2. It comprises of a hybrid  $\text{CO}_2$  laser oscillator and a UV preionized TEA  $\text{CO}_2$

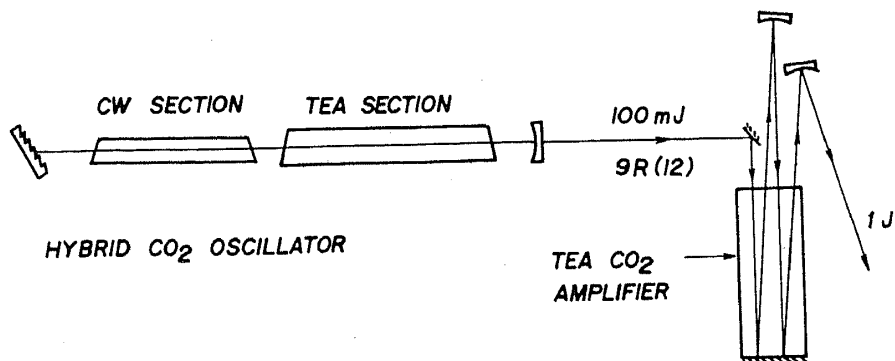


Figure 2. The CO<sub>2</sub> laser pump system.

amplifier. The line tunable, hybrid CO<sub>2</sub> laser oscillator, provided  $\sim 100$  mJ output at a single longitudinal mode near the line center of the 9  $\mu\text{m}$  R(12) line. This output was then amplified to  $\gtrsim 1$  J level by making four passes through the 45 cm long TEA CO<sub>2</sub> amplifier having a discharge cross section of 4  $\times$  4 cm. The beam configuration through the amplifier and the delay between the discharges of the oscillator and the amplifier were optimised for efficient energy extraction. The measured four pass gain of ten was in reasonable agreement with the theoretical estimates based on the configuration used.

A notable feature of the set up was the use of a polythene sheet as the optical window (Shikarkhane *et al* 1988) for the CO<sub>2</sub> amplifier because large aperture (10 cm diameter) conventional optical windows (required to make four passes through the amplifier) were not locally available. The polythene window did not result in any significant degradation of the beam quality of the amplified pulsed output. However, the cw CO<sub>2</sub> laser radiation could not be used for the alignment as it resulted in deformation of the window.

Long term operation of the CO<sub>2</sub> laser system revealed a gradual decay in the hybrid laser output at 9R(12) line. After an operational period of  $\sim 400$  h the hybrid laser output dropped to  $\sim 60\%$  of its initial value and more significantly the cw section of the hybrid oscillator could not be made to lase on the 9.6  $\mu\text{m}$  band lines. This was traced to be due to a gradual accumulation of some whitish 'deposits' on the ZnSe Brewster windows, especially the one at the cathode end of the cw discharge section. The deposits were resistant to normal cleaning methods and had an absorption band overlapping the 9  $\mu\text{m}$  CO<sub>2</sub> laser band. The usual window transmission was restored by lapping and repolishing the window. The gases were tested to be free from any contaminants to an impurity level of less than 1% by gas chromatographic analysis. The likely causes for the degradation of the optical quality of the ZnSe windows appear to be sputtering from the aluminium cathode, and laser induced thermochemical changes (Ursu *et al* 1986) which may be accelerated by the ambient humidity and dust. Increasing the distance of the ZnSe window from the cathode to  $\sim 15$  cm and leaving the cw cell in an inert atmosphere have helped improve the performance; the cw output has dropped by only a factor of two after 500 h of operation whereas previously it had stopped lasing after 400 h of operation. More detailed and careful measurements are required to find the exact mechanism for the gradual degradation in the optical quality of the window.

#### 4. $\text{CF}_4$ Cell

Most of the cryogenic cells (Tiee *et al* 1979; Bonanni *et al* 1981) used for  $\text{CF}_4$  laser have been cooled by liquid nitrogen boil off. Apart from an inefficient use of the cryogen (since the latent heat of vaporization is wasted) these cells have poor temperature uniformity. Temperature non-uniformity of up to  $30^\circ\text{K}$  over the cold length have been measured (Bonanni *et al* 1981). Better temperature uniformity is desirable because the most efficient laser operation occurs at the minimum temperature compatible with the required vapour pressure. Indeed, when operated on the saturated vapour pressure curve, an increase in operating temperature of only  $5^\circ\text{K}$  can result in a drop in  $\text{CF}_4$  laser output by a factor of two or three (Green 1979).

The design of a cryogenic cell which can provide temperature uniformity of a few  $^\circ\text{K}$  over the cold length is shown in figure 3. The cell which is similar to the one developed by Rutt (1985) consists of a 3 m long, 34 mm internal diameter copper tube on which were wound three segments of a teflon insulated heater. The three segments are of equal length ( $R = 120\ \Omega$ ) and connected to separate power supplies. The copper tube was placed in an annular stainless steel liquid nitrogen jacket (the inner and the outer diameters of the two tubes being 81; 89 mm and 128; 142 mm respectively). The liquid nitrogen tank was insulated from the atmosphere by two layers of 6 cm thick freon impregnated polyurethane foam moulded in semi-cylindrical form to fit the tube. Thermal insulation between the variable temperature copper tube and the liquid nitrogen bath was provided by filling the annular space between the two by vermiculite (expanded mica). The latter was purged with dry nitrogen to avoid condensation of atmospheric water vapour in the vermiculite which greatly increases its thermal conductivity. A chromel constantan thermocouple was attached to each of the three heater segments to monitor the cell temperature. Since the liquid nitrogen tank provides a reference temperature, by adjusting the power dissipated in the three heaters the cell temperature was varied from  $\sim 90^\circ\text{K}$  to  $\sim 230^\circ\text{K}$ . The power dissipated in three heaters was independently adjusted to ensure temperature uniformity over the cold length (inferred from the temperature measured at the three points where the thermocouples were located) of  $\sim 5^\circ\text{K}$ . The absence of any significant cold spots was ascertained by measurements of the saturated vapour pressure.

*Pumping arrangement.* A schematic diagram of the pumping arrangement used for  $\text{CF}_4$  laser is shown in figure 4. The  $\text{CO}_2$  laser radiation was injected in the cryogenic cell through a Ge Brewster window. The pump radiation was *p* polarized so as to transmit through the Brewster plate without reflection loss. Due to the constraints on the available optics only  $\sim 500\text{ mJ}$  of the  $\text{CO}_2$  laser radiation could be injected into the  $\text{CF}_4$  gas. The pump beam was gently focused in the centre of the cell to result in peak energy fluence of  $\sim 1\text{ J/cm}^2$ . The  $16\ \mu\text{m}$  laser cavity was formed for the orthogonal polarization by the mirror  $M_1$  and the output coupler connected through the reflection at the Brewster surface. Since large gain lengths are involved the  $\text{CF}_4$  laser can operate even without feed-back in the amplified spontaneous emission (ASE) mode (figure 4b, c). In the arrangement of figure 4c a fraction of the  $16\ \mu\text{m}$  radiation growing in the direction opposite to the pump beam is reflected back by the Ge Brewster window and the mirror  $M_2$  to add to the useful output from the other end of the cell. The  $16\ \mu\text{m}$  output was separated from the pump  $\text{CO}_2$  radiation via a combination of a LiF reststrahlen filter and a band pass dielectric filter. The latter

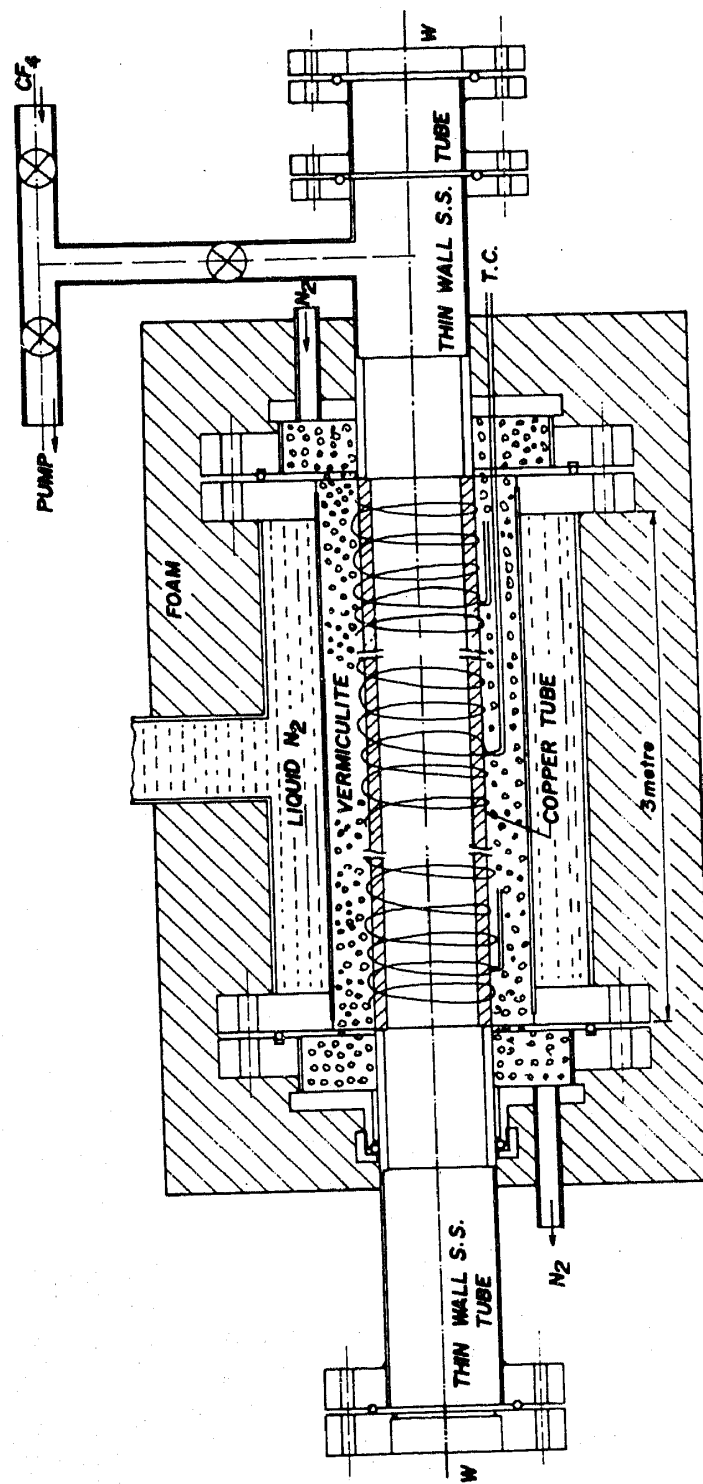


Figure 3. The cryogenic cell.

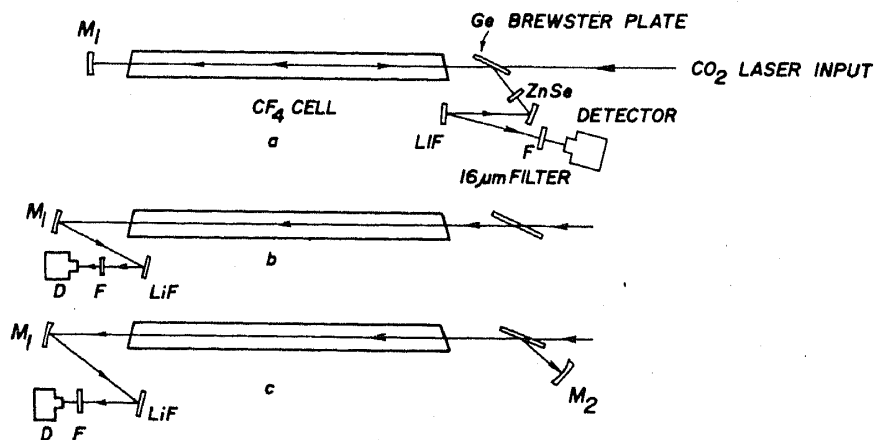


Figure 4. The pumping arrangements used for the  $\text{CF}_4$  laser.

had a high rejection for  $\text{CO}_2$  radiation and  $\sim 70\%$  transmission in the  $16\text{ }\mu\text{m}$  range. The combination provided a discrimination of  $10^6:1$  in favour of the  $16\text{ }\mu\text{m}$  radiation. A calibrated electron pyroelectric detector (J3-05) was used for  $16\text{ }\mu\text{m}$  energy measurements.

*$\text{CF}_4$  Laser characteristics.* The dependence of the  $\text{CF}_4$  laser output on the operating temperature and the gas pressure was investigated for the three configurations shown in figure 4. In figure 5 we show the measured pressure dependence of the  $\text{CF}_4$  laser output using the configuration 4c. The experimental points shown are average over several pulses and the bars show the per cent variation in the output ( $2\sigma/\bar{x}$ , where  $\sigma$  is the standard deviation and  $\bar{x}$  the average). The observed pressure dependence arises because the laser gain is a function of the operating pressure. It increases with pressure at low pressures (Doppler-broadened regime) due to the increase in the number density and in the pressure broadened region it becomes independent of pressure, the increase in the number density being offset by an increase in the bandwidth of the transition. The drop in output at the higher operating pressure is due to two reasons. First, the increasing loss introduced by the overlapping absorption band. Second, for higher pressures, the input pump intensity may also cease to be sufficient for inverting population over the entire gas column. In such a situation not only is the gain reduced but self absorption also increases due to the significant thermal population in the lower laser level. The reduction in self absorption at lower temperatures is responsible for the observed increase in the maximum operating pressure to  $\sim 15$  torr at  $115^\circ\text{K}$  from  $\sim 9$  torr at  $190^\circ\text{K}$ . The optimum operating pressure is seen to decrease slightly at the lower operating temperature. This is because maximum gain occurs at a pressure which decreases slowly with decreasing temperature as a result of the Doppler width of the lasing transition decreasing. Further the collisional broadening coefficient will also increase with reducing temperature because at constant pressure, the rotational relaxation time is expected to vary as  $T^{1/2}$  (Green 1979). It is also important to note in figure 5 that away from the optimum operating pressure (4–5 torr), the pulse to pulse variation in the laser energy output increases significantly. In particular,  $\text{CF}_4$  laser operation near the maximum operating pressure is very erratic with laser action occurring in one pulse out of 5–10 pump pulses. One important reason for this erratic behaviour is that the pump laser frequency is not

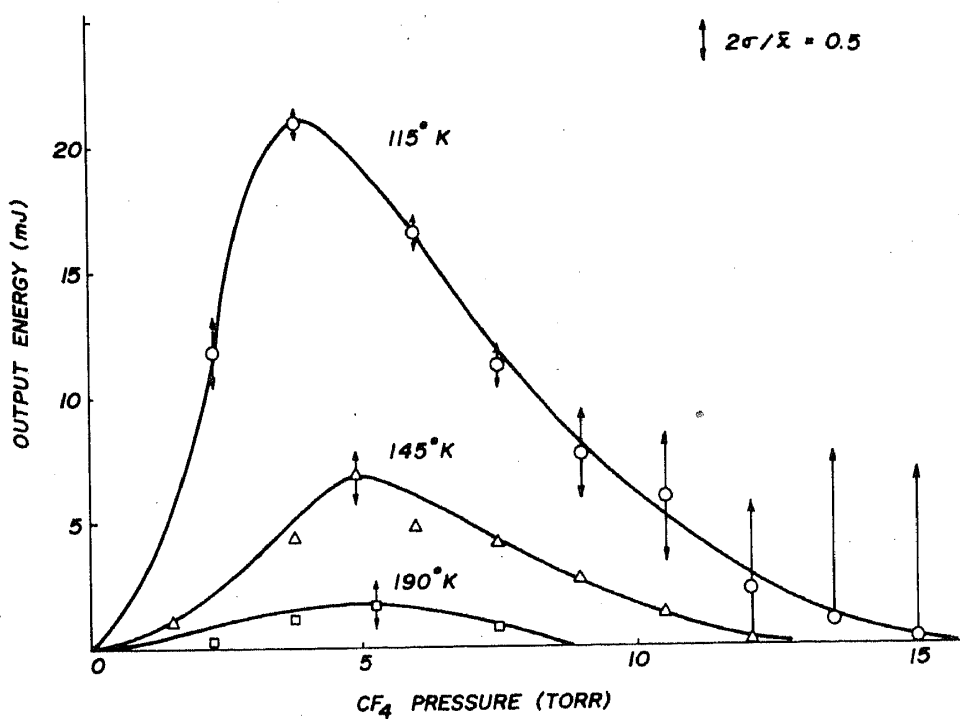


Figure 5. Output energy versus gas pressures at various temperatures for the 16  $\mu\text{m}$  CF<sub>4</sub> laser.

locked and can wander within the gain bandwidth of the low pressure section. The maximum frequency by which the pump laser frequency can get detuned for the CO<sub>2</sub> laser line center is by half the cavity mode spacing for the pump laser ( $\sim 50$  MHz). The resulting change in the absorbed energy and hence the gain at 16  $\mu\text{m}$  will lead to much larger changes in the laser amplitude for operation close to the lasing threshold and thus at pressures away from the optimum operating pressures. Better amplitude stability will require stabilization of the pump laser frequency to within  $\pm 5$  MHz (Hawkins *et al* 1985).

In figure 6 we show a plot of the CF<sub>4</sub> laser energy obtained at the optimum (temperature-dependent) pressure against the operating temperature. The output is seen to have a rather strong temperature dependence and increases by a factor of 40 on reduction in temperature from 228°K to 115°K. Under optimum conditions, 5 mJ output was obtained in the oscillator mode (figure 4a) with an uncoated ZnSe window as an output coupler. The energies obtained in the ASE mode were 15 mJ with the arrangement as in figure 4b (mirror  $M_2$  removed) and 20 mJ with the arrangement as in figure 4c. The increased output in the ASE mode is presumably due to the large gain lengths and the use of a lossy cavity for the oscillator (the intracavity Ge Brewster window reflects only 78% of the s polarized 16  $\mu\text{m}$  radiation). In our experiments only  $\sim 40\%$  of the CO<sub>2</sub> laser energy was absorbed in the gas column, under the optimum operating conditions ( $T = 115^\circ\text{K}$ ,  $P \sim 4$  torr). This implies an absorption cross-section, averaged over the pump laser bandwidth, of  $\sim 5.1 \times 10^{-21} \text{ cm}^2$  in reasonable agreement with the other reported values (Bonanni *et al* 1981). Thus in our experiments 20 mJ output is generated at 16  $\mu\text{m}$  with  $\sim 200$  mJ of the CO<sub>2</sub> laser energy absorbed in the gas. The resulting absorbed energy conversion efficiency of  $\sim 10\%$  compares favourably with the best reported values for this emission. (Barnov *et al* 1980; Stein *et al* 1978).

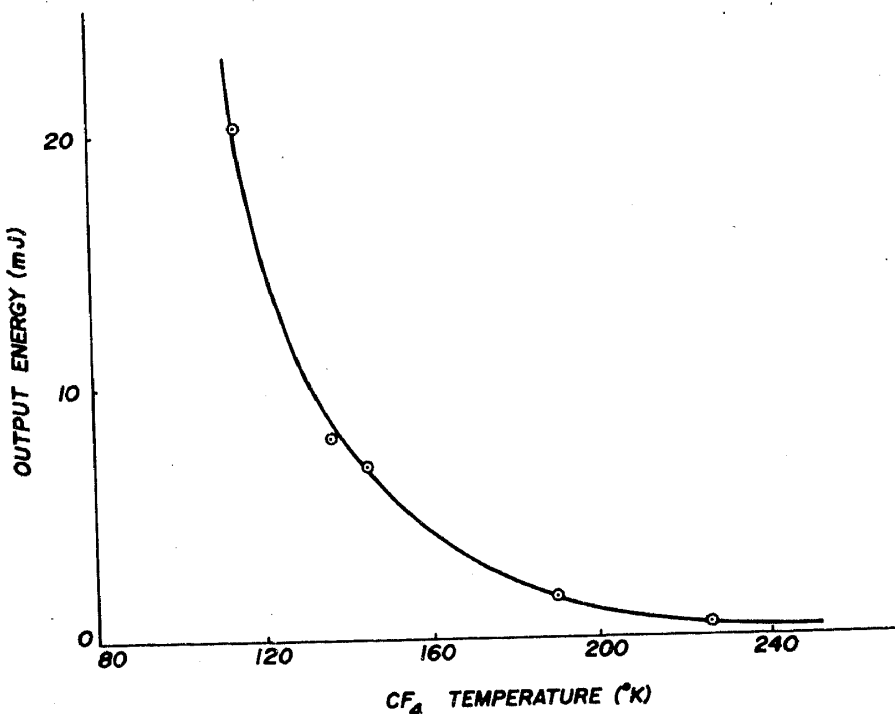


Figure 6. Maximum output energy versus gas temperature for the 16  $\mu\text{m}$  CF<sub>4</sub> laser.

## 5. Conclusion

To conclude, a CO<sub>2</sub> laser pumped CF<sub>4</sub> laser has been developed at BARC. Output energies of upto 20 mJ have been obtained with an absorbed energy conversion efficiency of  $\sim 10\%$ .

## Acknowledgement

The authors would like to thank Dr K C Rustagi, Dr P R K Rao, Dr J P Mittal and Dr D D Bhawalkar for their help and encouragement at various stages of work.

## References

- Ambartsumyan R V, Apatin V M, Basov N G, Grasyuk A Z, Dyad'kin A P, and Furzikov N P 1979 Sov. J. Quantum Electron. **9** 1546
- Barnov V Yu, Kazakov S A, Mezhekov V S, Napartovich A P, Orlov M Yu, Pis'mennyi V O, Starodubtsev A I and Starostin A I 1980 Sov. J. Quantum Electron. **10** 47
- Bonanni F, Castiglione S, and Salvetti G 1981 Nuovo Cimento **B66** 129
- Grasyuk A Z, Letokhov V S and Lobko V V 1981 Prog. Quantum Electron. **6** 245
- Green J M 1979 J. Phys. D. **12** 489
- Green J M, Stamatakis T and Aldcroft D A 1981 Opt. Commun. **39** 49
- Gupta P K and Mehandale S C 1987 Hyperfine Interactions **37** 243
- Hawkins K C, Peacock R and Rutt H N 1985 J. Phys. D **18** 191
- Horsley J A, Rabinovitz P, Stein A, Cox D M, Brickman R O and Kaldor A 1980 IEEE J. Quantum Electron. **OE-16** 412

Jones C R, Telle J M and Buchwald M I 1978 *Digest of technical papers presented at Tenth Int. Quantum Electron. Conf.* Atlanta, Publ. by Optical Soc. of America, Washington, D.C. paper K-7

Koren G, Gerther Y and Shreter U 1982 *Appl. Phys. Lett.* **41** 397

McDowell R S, Patterson C W, Jones C R, Buchwald M I and Telle J M 1979 *Opt. Lett.* **4** 274

Rutt H N 1985 *J. Phys. E* **18** 334

Shikarkhane N S, Nundy U and Chatterjee U K 1988 *Appl. Opt.* **27** 1636

Stamatakis T and Green J M 1979 *Opt. Commun.* **30** 413

Stein A, Rabinowitz P and Kaldor A 1978 *Opt. Lett.* **3** 97

Tiee J J and Wittig C 1978 *Opt. Commun.* **27** 377

Tiee J J, Fischer T A and Wittig C 1979 *Rev. Sci. Instrum.* **50** 958

Ursu I, Mihailescu I N, Nistor L C, Teodorescu V S, Prokhorov A M, Chapliev N I, Konov V I and Starodumov Yu M 1986 *Appl. Phys. A* **40** 227